

**Exotic nuclear shape due to cluster formation at high angular momentum**Balaram Dey,<sup>1,\*</sup> Shan-Shan Wang,<sup>2</sup> Deepak Pandit,<sup>3,†</sup> Srijit Bhattacharya,<sup>4</sup> Xi-Guang Cao,<sup>5,6,2,‡</sup> Wan-Bing He<sup>6,7</sup>, Yu-Gang Ma<sup>6,7,2</sup>, N. Quang Hung<sup>6,8,9</sup> and N. Dinh Dang<sup>6,10</sup><sup>1</sup>*Department of Physics, Bankura University, Bankura, West Bengal 722155, India*<sup>2</sup>*Shanghai Institute of Applied Physics, Chinese Academy of Sciences, Shanghai 201800, China*<sup>3</sup>*Variable Energy Cyclotron Centre, 1/AF Bidhan Nagar, Kolkata 700064, India*<sup>4</sup>*Department of Physics, Barasat Government College, Kolkata 700124, India*<sup>5</sup>*Shanghai Advanced Research Institute, Chinese Academy of Sciences, Shanghai 201210, China*<sup>6</sup>*Zhangjiang Laboratory, Shanghai 201210, China*<sup>7</sup>*Key Laboratory of Modern Physics and Ion-Beam application (MOE), Institute of Modern Physics, Fudan University, Shanghai 200433, China*<sup>8</sup>*Institute of Fundamental and Applied Sciences, Duy Tan University, Ho Chi Minh City 700000, Vietnam*<sup>9</sup>*Faculty of Natural Sciences, Duy Tan University, Da Nang City 550000, Vietnam*<sup>10</sup>*Quantum Hadron Physics Laboratory, RIKEN Nishina Center for Accelerator-Based Science, RIKEN, 2-1 Hirosawa, Wako City, Saitama 351-0198, Japan*

(Received 1 January 2020; revised 6 July 2020; accepted 3 August 2020; published 8 September 2020)

It is shown, for the first time, how the exotic shapes due to cluster formation at high excitation energy and angular momentum are manifested through giant dipole resonance (GDR) strength function under the framework of the extended quantum molecular dynamics (EQMD) model. The results of EQMD calculation are compared with the existing experimental data of  $^{32}\text{S}$  and  $^{28}\text{Si}$  formed in the reactions  $^{20}\text{Ne} + ^{12}\text{C}$  and  $^{16}\text{O} + ^{12}\text{C}$ , respectively, at high angular momenta. It is found that the EQMD predicts the general trend of the experimental GDR strength functions for  $^{32}\text{S}$  and  $^{28}\text{Si}$  by considering the ring or toroidal configuration, whereas the linear chain configurations with  $\alpha$  clusters can reproduce the higher-energy peak in  $^{32}\text{S}$  and  $^{28}\text{Si}$ . Thus, the direct signature of the cluster formation at high temperature and angular momentum is the observation of a GDR peak  $\approx 25$  MeV which cannot be predicted within the mean-field calculations. The present result highlights the role of  $\alpha$  cluster states above the decay threshold, which is still an open field of investigation.

DOI: [10.1103/PhysRevC.102.031301](https://doi.org/10.1103/PhysRevC.102.031301)

The basic building blocks of the atomic nucleus are protons and neutrons, known as nucleons. In general, the nucleonic matter behaves as a quantum fluid under the mean-field effect. However, in some cases, the atomic nuclei also display a moleculelike structure due to the mutual interaction of these nucleons [1,2]. The  $\alpha$  particle, formed from two protons and two neutrons by antialigning the spins of same nucleons to minimize the Pauli repulsion, has a much larger binding energy per nucleon than that of the other light nuclei. The second  $0^+$  state in  $^{12}\text{C}$ , the putative Hoyle state, which is the doorway for the synthesis of  $^{12}\text{C}$  in stellar nucleosynthesis, is predicted to exhibit a structure composed of three  $\alpha$  particles with a Bose-Einstein condensation picture [3–6]. Cluster radioactivity is another signature of clustering in the atomic nuclei [7,8]. Thus, clusterization is an indispensable feature of the nuclear many-body system which coexists with the nuclear mean field. It is very perplexing that, even though the formation of clusters of nucleons has been realized in

the earliest days of the nuclear physics study [9], the mechanism of clustering is not yet fully understood. According to the Ikeda diagram, cluster structures are predicted to appear close to the associated decay thresholds [10]. However, the influence of clustering in the structure of ground as well as excited states has also been reported for several  $\alpha$ -conjugate nuclei [11–16]. The search for such exotic behavior has been extended for light neutron-rich nuclei as well as for halo nuclei, such as  $^{11}\text{Li}$  [17] and  $^{14}\text{Be}$  [18]. The understanding of nuclear clustering is important to inculcate the intricate details of nuclear correlation in the miniscule atomic nucleus that could help us to probe even massive astronomical objects especially the internal structure of neutron stars—the crust made of nuclear “pasta.”

It is now well established [19–24] that clustering plays a very important role in self-conjugate light nuclei and is associated with strongly deformed shapes of nuclei. One of the probes to study this deformation experimentally at high temperature ( $T$ ) and angular momentum ( $J$ ) is the  $\gamma$  decay from the giant dipole resonance (GDR) built on excited states [25,26]. The GDR line shape gets fragmented in deformed nuclei providing crucial information about the nuclear deformation. As a matter of fact, it has been successfully

\*dey.balaram@gmail.com

†deepak.pandit@vecc.gov.in

‡caoxiguang@zjlab.org.cn

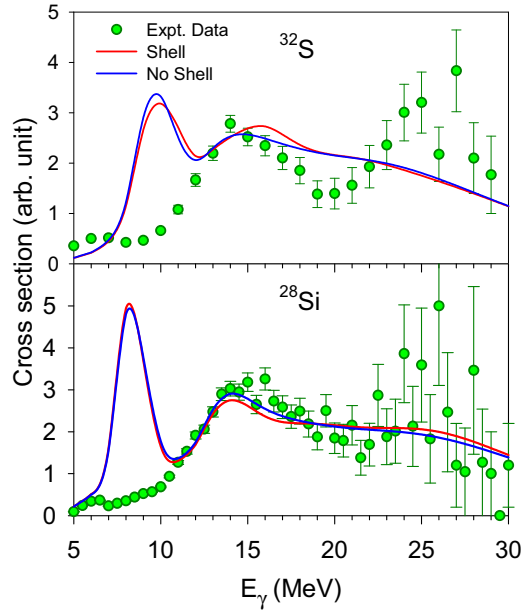


FIG. 1. Filled circles represent the linearized GDR strength functions for  $^{28}\text{Si}$  and  $^{32}\text{S}$  nuclei obtained from the best-fitted GDR parameters as reported in Refs. [27,31,32]. The lines represent the TSMF calculations with and without shell corrections.

employed experimentally to study the Jacobi shape transition, an abrupt change in shape from the noncollective oblate to the collective triaxial or prolate shape above a critical spin in several light nuclei, such as  $^{31}\text{P}$  [27],  $^{45}\text{Sc}$  [28],  $^{46}\text{Ti}$  [29,30], and  $^{47}\text{V}$  [31]. However, when this shape transition is examined in self-conjugate nuclei  $^{28}\text{Si}$  [27] and  $^{32}\text{S}$  [31,32] through the reactions  $^{16}\text{O} + ^{12}\text{C}$  and  $^{20}\text{Ne} + ^{12}\text{C}$ , respectively, the GDR line shape fragments into two prominent peaks at high  $J$  ( $\approx 20\hbar$ ) providing direct evidence of the large deformation but, intriguingly, the shapes found are completely different from those seen in the Jacobi shape transition (signature of which is a sharp peak at 10 MeV arises due to the Coriolis splitting of the GDR frequencies). Therefore, these observations clearly highlight that the clustering is not only important in the mass region  $A < 20$ , but also could play major role in  $A \approx 30$ , which has not been sufficiently studied enough. A recent experimental investigation reveals resonances at high excitation energy in the  $7\alpha$  disassembly of  $^{28}\text{Si}$  with very high angular momentum, which gives evidence for the population of toroidal high-spin isomers. The  $\alpha$  clusters play important roles in this abnormal resonance and decay [33,34].

Microscopic effects, such as shell structure, pairing, and isospin effects play important roles in deciding the nuclear structures at low excitation energy. However, even after incorporating these effects, the experimental GDR line shapes ( $T \approx 2.0$  MeV and  $J \approx 20\hbar$ ) could not be explained for  $^{28}\text{Si}$  and  $^{32}\text{S}$  nuclei. As can be seen from Fig. 1, the thermal shape fluctuation model [27,35–42] calculations (including and excluding shell effects), performed at similar  $T$  and  $J$  values, completely fail to describe the corresponding experimental GDR strength functions. The finite-temperature BCS (FTBCS) calculations [43,44] in Fig. 2 show that  $n$ - $n$  and

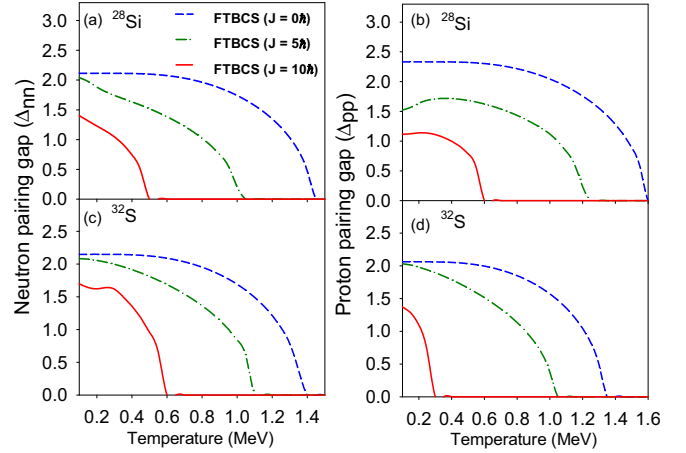


FIG. 2. Neutron ( $\Delta_{nn}$ ) and proton ( $\Delta_{pp}$ ) pairing gaps as functions of temperature at different angular momenta obtained within the FTBCS theory.

$p$ - $p$  pairing gaps vanish already at  $T \geq 0.6$  MeV for  $J = 10\hbar$ , negating the interference of pairing effects for the  $^{28}\text{Si}$  and  $^{32}\text{S}$  nuclei. It has also been observed that isospin is not conserved in these reaction channels [32].

In this Rapid Communication, we have investigated, for the first time, the GDR strength function of  $\alpha$ -cluster nuclei  $^{28}\text{Si}$  and  $^{32}\text{S}$  at high  $T$  and  $J$ , using the extended quantum molecular dynamics (EQMD) model. The EQMD calculations considering toroidal shape represent the general trend of the experimental data especially the peak at 25 MeV, which point towards the existence of exotic shapes of nuclei due to clusterization even at extreme conditions.

Recently, the EQMD model [45–47] modification of the idea of quantum molecular dynamics (QMD) [48–51] has been successfully applied to investigate the GDR. In this semiclassical framework, a phenomenological Pauli potential has been added with the effective interaction to approximate the nature of the fermionic many-body system and blocking effects. The width of each wave packet has also been treated within EQMD as an independent dynamical variable [52]. The ground state of initialized  $\alpha$ -cluster nuclei is insufficiently stable in the standard QMD model, whereas the EQMD model is able to consider the energy minimum states as initial ground states due to two aspect improvements. The first improvement is to include the Pauli potential into effective interactions. The other one is to take into account the kinetic-energy term of the momentum variance of wave packets in the Hamiltonian, which is neglected as the spurious constant term in the standard QMD [48,49]. These modifications not only describe the ground state better, but also make the model successful in the study of exotic nuclei, such as cluster structures. This improvement is necessary to describe the nuclear cluster states. Recently, the EQMD model has been successfully used in describing the GDR in light-cluster [45,46,53] and deformed [54] nuclei.

In the EQMD model, the wave function of the system is described as the direct product of the Gaussian wave packets

of all nucleons [52],

$$\Psi = \prod_i \varphi(\mathbf{r}_i), \quad (1)$$

$$\varphi(\mathbf{r}_i) = \left( \frac{v_i + v_i^*}{2\pi} \right)^{3/4} \exp \left[ -\frac{v_i}{2} (\mathbf{r}_i - \mathbf{R}_i)^2 + \frac{i}{\hbar} \mathbf{P}_i \cdot \mathbf{r}_i \right], \quad (2)$$

where  $\mathbf{R}_i$  and  $\mathbf{P}_i$  are the central positions of the  $i$ th wave packet in the coordinate and momentum spaces, respectively. The  $v_i$  term is the width of the wave packet which is defined as  $v_i \equiv 1/\lambda_i + i\delta_i$ . Both  $\lambda_i$  and  $\delta_i$  are dynamic variables.

The Hamiltonian is written as

$$\begin{aligned} H &= \langle \Psi | \sum_i -\frac{\hbar^2}{2m} \nabla_i^2 - \hat{T}_{c.m} + \hat{H}_{int} | \Psi \rangle \\ &= \sum_i \left[ \frac{\mathbf{P}_i^2}{2m} + \frac{3\hbar^2(1 + \lambda_i^2 \delta_i^2)}{4m\lambda_i} \right] - T_{c.m} + H_{int}, \quad (3) \end{aligned}$$

The equation of motion of nucleonic centroids and the width of the wave packet are determined by the time-dependent variational principle.

The effective interaction includes the Skyrme and Coulomb forces, the symmetry energy, and the Pauli potential,

$$H_{int} = H_{Skyrme} + H_{Coulomb} + H_{symmetry} + H_{Pauli}, \quad (4)$$

where the Pauli potential is written as

$$H_{Pauli} = \frac{c_p}{2} \sum_i (f_i - f_0)^\mu \theta(f_i - f_0). \quad (5)$$

with  $f_0 = 1.0$ ,  $\mu = 1.3$ ,  $f_i$  being the overlap of a nucleon  $i$  with the same spin and isospin of nucleons and  $c_p = 15$  MeV denoting the strength of the potential.  $f_i \equiv \sum_{j=1}^A \delta(S_i, S_j) \delta(T_i, T_j) |\langle \varphi_i | \varphi_j \rangle|^2$ , where  $A$ ,  $S_i$ ,  $T_i$ , and  $\varphi_i$  are the mass number of the system, spin, isospin, wave function of the  $i$ th nucleon, respectively.  $\theta(f_i - f_0)$  is the unit step function.

According to the macroscopic description of the GDR given by the Goldhaber-Teller model, which assumes that protons and neutrons collectively oscillate along opposite directions [55], the dipole moments of the system in the coordinate  $D_G(t)$  space can be written as [45,46,54,56–58]

$$D_G(t) = \frac{NZ}{A} [R_Z(t) - R_N(t)], \quad (6)$$

where  $R_Z(t)$  and  $R_N(t)$  are the center of mass of the protons and neutrons in the coordinate space, respectively.  $A$  is the sum of mass numbers of the target and projectile nuclei.  $N$  and  $Z$  are the neutron and the proton numbers of the compound system, respectively. The  $\alpha$ -cluster nucleus is excited by nuclear collision, and, in the excited nucleus, neutrons and protons are not in the same position contributing to the dipole strength. In this Rapid Communication, the phase space of the compound nucleus in the fusion reaction is obtained by using the EQMD model. The  $\gamma$ -emission probability of the compound nuclear system at energy  $E_\gamma$  can be derived from Eq. (6) [59] as

$$\frac{dP}{dE_\gamma} = \frac{2e^2}{3\pi \hbar c^3 E_\gamma} |D''(\omega)|^2, \quad (7)$$

where  $D''(\omega)$  is obtained from the Fourier transform of the second derivative of  $D_G(t)$  with respect to time, i.e.,

$$D''(\omega) = \int_{t_1}^{t_2} D_G''(t) e^{i\omega t} dt, \quad (8)$$

where  $t_2 - t_1 = 200$  fm/c. This duration time is comparable with the typical giant resonance period derived from the  $\sim 7-8$  MeV width in  $^{32}\text{S}$  and  $^{28}\text{Si}$ . Note that we just take into account the GDR spectra of the compound nucleus in the reaction plane for the events without the nucleon emission under the condition that the compound nucleus rotates quickly during the evolution.

It is known that the incident projectile and target structures play an important role in forming the compound nuclei with the exotic shapes. The slow dynamical process and moderate excitation energy in the fusion reaction are very advantageous to form typical cluster structures in  $\alpha$ -conjugate projectile and target. Recent experiments and theoretical calculations show clustering effects playing an important role in the collisions between  $\alpha$ -conjugate nuclei [60]. Various microscopic models, such as time-dependent Hartree-Fock [61], time-dependent density functional theory [62], and QMD, etc., all reveal that, nucleon rearrangement occurs during the dynamical process of projectile and target approaching. Nucleon rearrangement helps the projectile/target with the cluster component in their ground state to develop a typical cluster configuration with exotic configuration in the low-lying excited state. In addition, the polarization can lead clusters to align on the reaction plane defined by the projectile and target. Aligning plays a crucial role to form the exotic configurations in the  $\alpha$ -conjugate nuclear collision, such as the famous  $0_2^+ - 0_2^+$  molecular state discovered in the  $^{12}\text{C} + ^{12}\text{C}$  collision [63]. The probability of forming exotic shapes is larger in the aligned collisions than in the real collision events consisting of various random incident orientations. However, in real collisions, the cluster degree of freedom in  $\alpha$ -conjugate nuclei can easily be manifested due to the excitation before the projectile and target touching. Therefore, in order to mimic the nucleon rearrangement and aligning mechanism, we made a reasonable hypothesis that the nucleon rearrangement and cluster polarization mechanism occur before the projectile and target touching each other. This hypothesis is well based on the cluster resonances with exotic configurations found in experiments and theoretical simulations of reactions between  $\alpha$ -conjugate projectiles and targets in the low-energy region.

It was observed that the ring (toroidal) and linear chain emerge as the main configurations in the aligned collisions within the EQMD calculations. The lifetime of the linear chain and ring has been calculated by using EQMD and found in agreement with the dynamical duration of heavy-ion collisions. These exotic configurations are driven by the collisions dynamics especially by the high angular momentum at the peripheral and semiperipheral collisions with the emergence of the  $\alpha$  degree of freedom. The  $20\hbar$  angular momentum for  $^{20}\text{Ne} + ^{12}\text{C}$  collisions and  $21\hbar$  angular momentum for  $^{16}\text{O} + ^{12}\text{C}$  collisions are set as input parameters in the EQMD calculations, respectively. The temperature measures both the random thermal motions of the  $\alpha$  cluster and how the

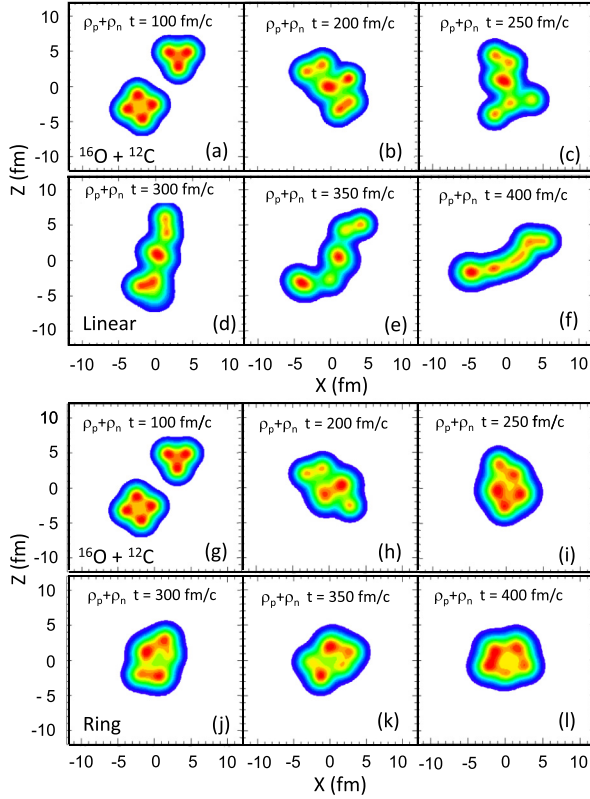


FIG. 3. Density distribution obtained within the EQMD calculations for the linear and ring shapes before and after the  $^{16}\text{O} + ^{12}\text{C}$  reaction, considering  $^{12}\text{C}$  as a triangle and  $^{16}\text{O}$  as a square.

$\alpha$  cluster deviates from the ideal linear chain and toroidal configurations. It is found that the temperature of the toroidal and linear chain configurations oscillates around 2 MeV during the GDR evolution, which is very close to the experimental temperature. The oscillation of the temperature is mainly from the rotational energy variation due to the dynamical shape fluctuation. It should be mentioned that there is a possibility of having  $^{16}\text{O} - ^{16}\text{O}$  cluster shapes in  $^{32}\text{S}$ . However, this possibility is much smaller than the configuration made of  $\alpha$ -cluster because the dynamical duration time of  $^{16}\text{O} - ^{16}\text{O}$  is much shorter than that of exotic shapes made of  $\alpha$ -cluster degrees of freedom.

In the case of the  $^{16}\text{O} + ^{12}\text{C}$  reaction, the EQMD calculations have been performed by considering different clustering structures of the  $^{12}\text{C}$  target (chain and triangle) and the  $^{16}\text{O}$  incident projectile (square and tetrahedral). In the case of the  $^{20}\text{Ne} + ^{12}\text{C}$  reaction, the projectile  $^{20}\text{Ne}$  has been taken as pentagonal and square pyramidal, whereas the target  $^{12}\text{C}$  has been considered as a triangle and chain. The alignment of the projectile and target is taken on the XZ plane. The density distribution before the collision considering the triangle shape for  $^{12}\text{C}$  and the square shape for  $^{16}\text{O}$  is displayed in Fig. 3 whereas the density distribution before the collision considering the triangle shape for  $^{12}\text{C}$  and pentagonal shape for  $^{20}\text{Ne}$  is displayed in Fig. 4. The dynamical fluctuation embedded in the QMD model is responsible for the different evolution paths leading to chain and toroidal configurations,

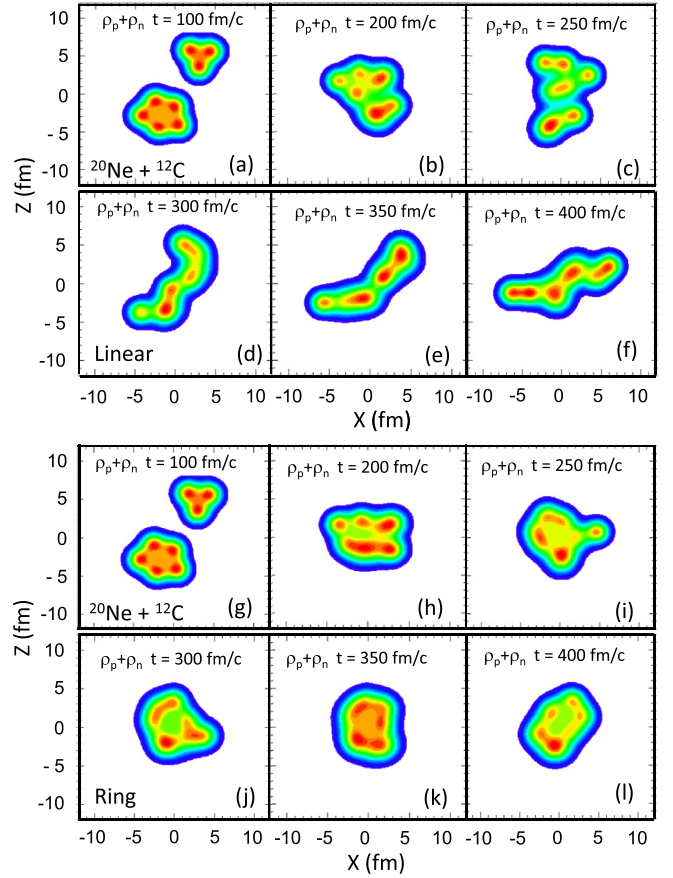


FIG. 4. Density distribution obtained within the EQMD calculations for the linear and ring shapes before and after the  $^{20}\text{Ne} + ^{12}\text{C}$  reaction, considering  $^{12}\text{C}$  as a triangle and  $^{20}\text{Ne}$  as a pentagonal.

even though the initial density distributions are the same. The density distributions of exotic toroidal and linear chain shapes formed in the reaction due to the peripheral collision for  $^{28}\text{Si}$  and  $^{32}\text{S}$  are also shown in Figs. 3 and 4, respectively. It was observed that the GDR line shape was split for both the final configurations (linear chain and toroidal) shown in Fig. 5. The double-peak structure originates due to the symmetric axial deformation of the nuclei, specifically, contributed by the coherent motion along the long and the short axes of the system. The toroidal and chain events both have peaks around 25 MeV, which are contributed by the coherence of transverse motion along the short axis of the system, namely, from the  $\alpha$  cluster. However, the general trend of the experimental data is represented well by the toroidal shape (ring) for both nuclei (shown in Fig. 5). The low-energy peaks in Figs. 5(a) and 5(c) are from the in-plane dipole oscillations, whereas the high-energy peaks are from the oscillations perpendicular to the circle plane. The high-energy peak manifests the  $\alpha$ -cluster degrees of freedom whereas the low-energy one embodies the compound nuclear size or configurations. It is also checked that the GDR line shapes obtained from the EQMD are nearly similar for all the initial target-projectile configurations pointing towards the fact that the GDR line shape is not affected by



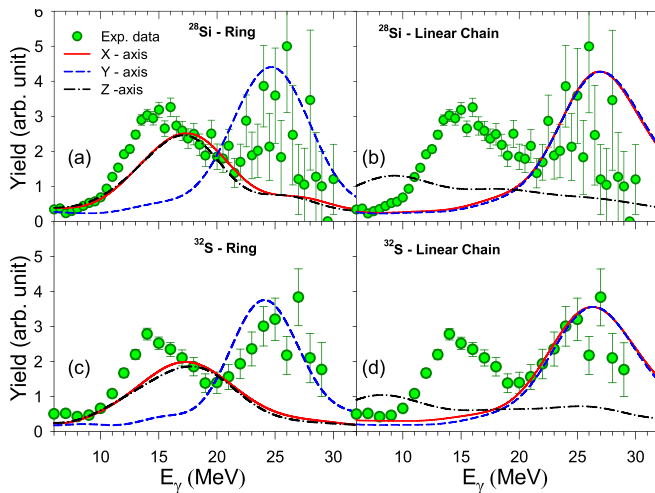


FIG. 5. The EQMD calculations for both  $^{28}\text{Si}$  and  $^{32}\text{S}$  nuclei are shown along with experimental data.

the initial clustering configuration of the projectile and target and depends only on the exotic shapes of compound systems.

It needs to be mentioned, here, that the GDR line shape should be the weighted sum of the various collision events with different incident configurations. However, it is difficult to weight the various collision events with different incident configurations since the dynamical nucleon arrangement and polarization mechanism occur to some larger content. Moreover, it is also not possible experimentally to disentangle the contribution of mean-field and clustering effects to the GDR line shape. Nevertheless, the peak around 25 MeV can only arrive due to cluster formation (as seen for both the linear chain and the toroidal configurations) highlighting the existence of the  $\alpha$ -clustering structure at such high  $T$  and  $J$  since this peak could not be predicted within the mean-field calculations (Fig. 1). Interestingly, the rotation of these exotic shapes will not lead to the Coriolis splitting of the GDR strength function (due to larger moment of inertia leading to smaller angular frequency), which could be the reason for the absence of the Jacobi shape transition in  $^{32}\text{S}$  and  $^{28}\text{Si}$  [27,31,32], even if they

were populated beyond the critical angular momentum. The present Rapid Communication, thus, provides a doorway to study the exotic shapes of nuclei due to the cluster formation above the  $\alpha$ -decay threshold. It is expected to play an important role in the cluster nucleosynthesis diagram [64] as well as in the Ikeda diagram [10] and may lead to the understanding of different stellar phenomena, such as the type-II supernova burning.

To summarize, the present Rapid Communication reveals, for the first time, how cluster shapes of nuclei ( $^{32}\text{S}$  and  $^{28}\text{Si}$ ) are manifested in the GDR strength function at high angular momentum ( $\approx 20\hbar$ ) and temperature ( $\approx 2$  MeV) under the framework of an extended quantum molecular dynamics model. It is found that the EQMD model (with exotic toroidal configurations) could predict the general trend of experimental GDR strength function of those nuclei built on high excitations. This Rapid Communication highlights that the observation of a GDR peak  $\approx 25$  MeV is direct evidence of the  $\alpha$ -cluster formation at these extreme conditions ( $J \approx 20\hbar$ ,  $T \approx 2.0$  MeV). In light of the success for explaining the splitting of GDR strength functions of  $^{32}\text{S}$  and  $^{28}\text{Si}$  by the EQMD model, it is expected that the GDR line shape of  $\alpha$ -conjugate nuclei at high temperature and angular momentum can reveal the exotic  $\alpha$ -cluster structure and their existence extremity.

We would like to thank Dr. S. R. Banerjee for useful discussions. X.-G.C. acknowledges the National Natural Science Foundation of China under Contracts No. U1832129, the Youth Innovation Promotion Association CAS (No. 2017309), and the National Key R & D Program of China under Contract No. 2018YFA0404404 and the Strategic Priority Research Program of the CAS under Grant No. XDB34030000. Y.-G.M. acknowledges the National Natural Science Foundation of China under Contracts No. 11890714 and No. 11421505, and the Key Research Program of the Chinese Academy of Sciences, Grant No. XDPB09-02. N.Q.H. and N.D.D. acknowledge financial support from the National Foundation for Science and Technology Development (NAFOSTED) of Vietnam through Grant No. 103.04-2019.371.

- [1] W. von Oertzen, M. Freer, and Y.-K. Enyö, *Phys. Rep.* **432**, 43 (2006).
- [2] M. Freer, *Rep. Prog. Phys.* **70**, 2149 (2007).
- [3] F. Hoyle, *Astrophys. J. Suppl. Ser.* **1**, 121 (1954).
- [4] T. K. Rana *et al.*, *Phys. Rev. C* **88**, 021601(R) (2013).
- [5] M. Freer and H. O. U. Fynbo, *Prog. Part. Nucl. Phys.* **78**, 1 (2014).
- [6] A. Tohsaki, H. Horiuchi, P. Schuck, and G. Röpke, *Phys. Rev. Lett.* **87**, 192501 (2001).
- [7] H. J. Jones and G. A. Jones, *Nature (London)* **307**, 245 (1984).
- [8] M. Warda and L. M. Robledo, *Phys. Rev. C* **84**, 044608 (2011).
- [9] John A. Wheeler, *Phys. Rev.* **52**, 1107 (1937).
- [10] K. Ikeda, N. Takigawa, and H. Horiuchi, *Prog. Theor. Phys. (Suppl.)* **E68**, 464 (1968).
- [11] Y. Liu and Y.-L. Ye, *Nucl. Sci. Tech.* **29**, 184 (2018).
- [12] P. Arumugam, B. K. Sharma, S. K. Patra, and Raj K. Gupta, *Phys. Rev. C* **71**, 064308 (2005).
- [13] J. A. Maruhn, Masaaki Kimura, S. Schramm, P.-G. Reinhard, H. Horiuchi, and A. Tohsaki, *Phys. Rev. C* **74**, 044311 (2006).
- [14] R. K. Gupta, in *Clusters in Nuclei*, edited by C. Beck, Lecture Notes in Physics Vol. 818 (Springer, Berlin, Heidelberg, 2010), pp. 223–265.
- [15] T. Ichikawa, J. A. Maruhn, N. Itagaki, and S. Ohkubo, *Phys. Rev. Lett.* **107**, 112501 (2011).
- [16] M. Barbui, K. Hagel, J. Gauthier *et al.*, *Phys. Rev. C* **98**, 044601 (2018).
- [17] K. Ikeda *et al.*, in *Clusters in Nuclei*, edited by C Beck, Lecture Notes in Physics Vol. 818 (Springer, Berlin, Heidelberg, 2010), pp. 165–221.

- [18] T. Nakamura and Y. Kondo, in *Clusters in Nuclei*, Vol. 2, edited by C. Beck, Lecture Notes in Physics Vol. 848 (Springer, Berlin, Heidelberg, 2012), pp. 67–119.
- [19] M. Kimura and H. Horiuchi, *Phys. Rev. C* **69**, 051304(R) (2004).
- [20] S. Ohkubo and K. Yamashita, *Phys. Rev. C* **66**, 021301(R) (2002).
- [21] D. Shapira, J. L. C. Ford Jr., J. Gomez del Campo, R. G. Stokstad, and R. M. DeVries, *Phys. Rev. Lett.* **43**, 1781 (1979).
- [22] S. J. Sanders, A. Szanto de Toledo, and C. Beck, *Phys. Rep.* **311**, 487 (1999).
- [23] C. Bhattacharya, A. Dey, S. Kundu, K. Banerjee, S. Bhattacharya, S. Mukhopadhyay, D. Gupta, T. Bhattacharjee, S. R. Banerjee, S. Bhattacharyya, T. Rana, S. K. Basu, R. Saha, S. Bhattacharjee, K. Krishan, A. Mukherjee, D. Bandopadhyay, and C. Beck, *Phys. Rev. C* **72**, 021601(R) (2005).
- [24] A. Dey, S. Bhattacharya, C. Bhattacharya, K. Banerjee, T. K. Rana, S. Kundu, S. Mukhopadhyay, D. Gupta, and R. Saha, *Phys. Rev. C* **74**, 044605 (2006).
- [25] M. N. Harakeh and A. van der Woude, *Giant Resonances, Fundamental High-Frequency Modes of Nuclear Excitation* (Clarendon, Oxford, 2001).
- [26] J. J. Gaardhoje, *Annu. Rev. Nucl. Part. Sci.* **42**, 483 (1992).
- [27] B. Dey *et al.*, *Phys. Rev. C* **97**, 014317 (2018).
- [28] M. Kicinska-Habior *et al.*, *Phys. Lett. B* **308**, 225 (1993).
- [29] A. Maj *et al.*, *Nucl. Phys. A* **731**, 319 (2004).
- [30] D. R. Chakrabarty, V. M. Datar, S. Kumar, G. Mishra, E. T. Mirgule, A. Mitra, P. C. Rout, V. Nanal, D. Pandit, S. Mukhopadhyay, and S. Bhattacharya, *Phys. Rev. C* **85**, 044619 (2012).
- [31] D. Pandit *et al.*, *Phys. Rev. C* **81**, 061302(R) (2010).
- [32] D. Pandit, D. Mondal, B. Dey, S. Bhattacharya, S. Mukhopadhyay, S. Pal, A. De, and S. R. Banerjee, *Phys. Rev. C* **95**, 034301 (2017).
- [33] X. G. Cao, E. J. Kim, K. Schmidt *et al.*, in *Proceedings of the 4th International Workshop on “State of the Art in Nuclear Cluster Physics” (SOTANCP4)*, edited by M. Barbui, C. M. Folden III, V. Z. Goldberg, and G. V. Rogachev, AIP Conf. Proc. No. 2038 (AIP, New York, 2018), p. 020021.
- [34] X. G. Cao, E. J. Kim, K. Schmidt *et al.*, *Phys. Rev. C* **99**, 014606 (2019).
- [35] M. Gallardo *et al.*, *Phys. Lett. B* **191**, 222 (1987).
- [36] J. M. Pacheco, C. Yannouleas, and R. A. Broglia, *Phys. Rev. Lett.* **61**, 294 (1988).
- [37] A. L. Goodman, *Nucl. Phys. A* **528**, 348 (1991).
- [38] N. Dubray, J. Dudek, and A. Maj, *Acta Phys. Pol., B* **36**, 1161 (2005).
- [39] Y. Alhassid, B. Bush, and S. Levit, *Phys. Rev. Lett.* **61**, 1926 (1988).
- [40] W. E. Ormand, P. F. Bortignon, and R. A. Broglia, *Phys. Rev. Lett.* **77**, 607 (1996).
- [41] D. Pandit, S. Bhattacharya, D. Mondal, B. Dey, S. Mukhopadhyay, S. Pal, A. De, and S. R. Banerjee, *Phys. Rev. C* **99**, 024315 (2019).
- [42] A. K. Rhine Kumar, P. Arumugam, and N. D. Dang, *Phys. Rev. C* **90**, 044308 (2014).
- [43] N. Q. Hung and N. D. Dang, *Phys. Rev. C* **84**, 054324 (2011).
- [44] N. Q. Hung, N. D. Dang, and L. G. Moretto, *Rep. Prog. Phys.* **82**, 056301 (2019).
- [45] W. B. He, Y. G. Ma, X. G. Cao, X. Z. Cai, and G. Q. Zhang, *Phys. Rev. Lett.* **113**, 032506 (2014).
- [46] W. B. He, Y. G. Ma, X. G. Cao, X. Z. Cai, and G. Q. Zhang, *Phys. Rev. C* **94**, 014301 (2016).
- [47] S. S. Wang *et al.*, *Nucl. Phys. Rev.* **32**, 24 (2015).
- [48] J. Aichelin and H. Stocker, *Phys. Lett. B* **176**, 14 (1986).
- [49] C. Hartnack *et al.*, *Eur. Phys. J. A* **1**, 151 (1998).
- [50] Z. Feng, *Nucl. Sci. Tech.* **26**, S20512 (2015).
- [51] J. Chen, Z. Q. Feng, and J. S. Wang, *Nucl. Sci. Tech.* **27**, 73 (2016).
- [52] T. Maruyama, K. Niita, and A. Iwamoto, *Phys. Rev. C* **53**, 297 (1996).
- [53] W. B. He *et al.*, *Nucl. Tech. (in Chinese)* **37**, 100511 (2014).
- [54] S. S. Wang, Y. G. Ma, X. G. Cao, W. B. He, H. Y. Kong, and C. W. Ma, *Phys. Rev. C* **95**, 054615 (2017).
- [55] M. Goldhaber *et al.*, *Phys. Rev.* **74**, 1046 (1948).
- [56] H. L. Wu, W. D. Tian, Y. G. Ma, X. Z. Cai, J. G. Chen, D. Q. Fang, W. Guo, and H. W. Wang, *Phys. Rev. C* **81**, 047602 (2010).
- [57] C. Tao, Y. G. Ma, G. Q. Zhang, X. G. Cao, D. Q. Fang, and H. W. Wang, *Phys. Rev. C* **87**, 014621 (2013).
- [58] V. Baran, M. Cabibbo, M. Colonna, M. Di Toro, and N. Tsoneva, *Nucl. Phys. A* **679**, 373 (2001).
- [59] V. Baran, D. M. Brink, M. Colonna, and M. Di Toro, *Phys. Rev. Lett.* **87**, 182501 (2001).
- [60] K. Schmidt, X. Cao, E. J. Kim *et al.*, *Phys. Rev. C* **95**, 054618 (2017).
- [61] C. Simenel, *Eur. Phys. J. A* **48**, 152 (2012).
- [62] B. Schuetrumpf and W. Nazarewicz, *Phys. Rev. C* **96**, 064608 (2017).
- [63] A. H. Wuosmaa, R. R. Betts, B. B. Back, M. Freer, B. G. Glagola, Th. Happ, D. J. Henderson, P. Wilt, and I. G. Bearden, *Phys. Rev. Lett.* **68**, 1295 (1992).
- [64] S. Kubono *et al.*, *J. Phys.: Conf. Ser.* **436**, 012071 (2013).